Biochimica et Biophysica Acta, 647 (1981) 18–28
Elsevier/North-Holland Biomedical Press

BBA 79368

PHASE TRANSITIONS OF THE PURPLE MEMBRANE AND THE BROWN HOLO-MEMBRANE

X-RAY DIFFRACTION, CIRCULAR DICHROISM SPECTRUM AND ABSORPTION SPECTRUM STUDIES

KENJI HIRAKI [a], TOSHIAKI HAMANAKA [a], TOSHIO MITSUI [a] and YUJI KITO [b]

[a] *Department of Biophysical Engineering, Faculty of Engineering Science, Osaka University, Toyonaka, Osaka 560 and*
[b] *Department of Biology, Faculty of Science, Osaka University, Toyonaka, Osaka 560 (Japan)*

(Received May 7th, 1981)

Key words: Bacteriorhodopsin; Purple membrane; Phase transition; X-ray diffraction

The phase transition of the purple membrane observed by differential scanning calorimetry (Jackson, M.B. and Sturtevant, J.M. (1978) Biochemistry 17, 911–915) has been investigated by X-ray diffraction, circular dichroism and absorption spectrum, in comparison with the phase transition in the brown holo-membrane. The two-dimensional crystal of bacteriorhodopsin transformed into two-dimensional liquid around 74–78°C in the purple membrane and around 50–60°C in the brown holo-membrane. The X-ray diffraction patterns obtained at 78°C for the purple membrane and at 60°C for the brown holo-membrane exhibit several broad peaks. Analysis of the pattern suggests that bacteriorhodopsin molecules aggregate in trimers even above the phase transition temperature. The negative circular dichroism band in the visible region is still present at 80°C in the purple membrane and at 60°C in the brown holo-membrane, but becomes negligibly small at 70°C in the brown holo-membrane. The 560 nm absorption peak due to bacteriorhodopsin changes its position and height drastically around 80°C in the brown holo-membrane as in the purple membrane. X-ray diffraction studies have been made on membranes of total lipids extracted from the purple membrane. No indication of the phase transition has been found between −81°C and 77°C.

Introduction

Halobacterium halobium cells produce the purple membrane, which sometimes occupy more than 50% of the cell membrane when cultured under limited oxygen supply [1–3]. Bacteriorhodopsin molecules form a two-dimensional hexagonal lattice with the space group p3 in the purple membrane [4,5]. The cells grown in the presence of nicotine (nicotine cells) are inhibited from synthesizing retinal but produce the chromophore-free apo-protein, bacterioopsin [6]. Bacterioopsin molecules are localized in the differentiated domains of the cell membrane, which are fractionated as membrane patches. The membranes in this fraction contain, in addition to bacterioopsin, cytochrome *b*-type protein as well as other minor protein species [6]. They will be called brown apo-membrane below following Papadopoulos and Cassim [7] to distinguish them from the brown membrane which is produced in the cells in the absence of nicotine. Addition of all-*trans* retinal to the brown apo-membrane fraction results in appearance of the characteristic absorption band of bacteriorhodopsin [8]. The membrane which is prepared from the brown apo-membrane by addition of retinal will be called brown holo-membrane below. Bacteriorhodopsin in it forms a two-dimensional hexagonal lattice with the cell edge of 6.3 nm (63 Å) as in the purple membrane [9].

Although the purple membrane and the brown holo-membrane give the X-ray diffraction pattern of

Abbreviation: DSC, differential scanning calorimetry.

the same type, there are some differences between them. The purple membrane patch has a continuous lattice throughout patch [10] and bacteriorhodopsin is immobilized in the crystalline lattice [11], whereas bacteriorhodopsin exhibits rotational motion around the normal to the plane of the membrane in the brown holo-membrane [12]. Also the rate of the light-dark adaptation of the brown holo-membrane is greater than that of the purple membrane [7,13].

Recently, Jackson and Sturtevant [14] have found with differential scanning calorimetry (DSC) that a small endothermic transition occurred in the purple membrane at about 80°C and a large one at 100°C. The 100°C transition is the irreversible denaturation of bacteriorhodopsin. The smaller 80°C transition is interpreted as a cooperative change in crystalline structure of the membrane. In the present study we have investigated the 80°C transition of the purple membrane and the phase transition of the brown holo-membrane by X-ray diffraction, circular dichroism (CD) and the absorption spectra. We have also examined the thermal behaviour of lipids extracted from the purple membrane by X-ray diffraction.

Materials and Methods

1. Specimen preparation.

(a) Purple membrane. Strain *Halobacterium halobium* R_1M_1 (kindly supplied by Dr. W. Stoeckenius) was grown under illumination and limited aeration at 37°C. Cells were harvested in the stationary state. Purple membrane was isolated according to the standard method of Oesterhelt and Stoeckenius [15].

(b) Brown apo-membrane and brown holo-membrane. Cells of *H. halobium* R_1M_1 were cultured in the presence of 1.5 mM nicotine. The brown apo-membrane was fractionated as described by Sumper and Herrmann [8]. Bacterioopsin was transformed to bacteriorhodopsin by addition of all-*trans* retinal to brown apo-membrane [8,12,13,16]. The brown apo-membrane was dispersed in 20 mM Tris-HCl buffer (pH 7.4). Fig. 1A shows absorption spectra before (a) and after (b) the retinal addition. The absorbance at 560 nm due to bacteriorhodopsin is much higher than the Soret band at 415 nm due to cytochrome *b*-type protein, suggesting that bacteriorhodopsin is the major protein in the membrane. We have determined

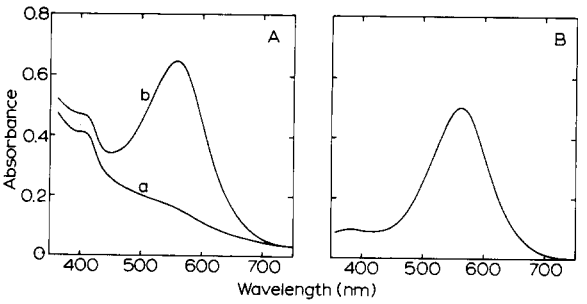

Fig. 1. A. Absorption spectra of the brown apo-membrane (a) and the dark-adapted brown holo-membrane (b). B. Difference spectrum, b – a in A.

the molar ratio of bacterioopsin/cytochrome *b*-type protein in the brown apo-membrane by SDS-polyacrylamide gel electrophoresis and by the method of Lowry et al. [17] with the corrections proposed by Rehorek and Heyn [18]. In the calculation, existence of minor proteins was neglected. Both methods gave the ratio 5 ~ 6. The Soret band shifted from 415 nm to 425 nm by reduction of cytochrome with sodium dithionite as reported in the reference [8]. Fig. 1B shows the difference between the two curves in Fig. 1A. The small bump around 380 nm indicates existence of excess retinal.

(c) Preparation of oriented membranes. Oriented specimens were used for X-ray studies since they give the in-plane diffractions separately from others. Membranes dispersed in distilled water were pelleted by centrifugation and partially dried on a thin-aluminium sheet (17 μm thickness) under controlled relative humidity, by using saturated $ZnSO_4 \cdot 7H_2O$ solution (90%, 20°C) [19]. Specimens thus prepared will be called a partially hydrated specimen below. To prepare a fully hydrated oriented specimen a strip of about 1 mm width was cut off from the partially hydrated specimen and immersed in distilled water for a few seconds. The specimen was found swollen due to the infiltration of water into inter-membrane space. This hydrated strip was sealed in a thin-wall glass capillary (wall-thickness was 10 μm) with a small amount of water at a different position for X-ray studies.

(d) Thermally denatured purple membrane. The purple membrane dispersed in distilled water was incubated in boiling water until the purple colour irreversibly lost. Upon cooling back to room tempera-

ture, the oriented specimen was prepared as described in (c).

(e) Lipid membrane. Lipids were extracted from the purple membrane by the method of Kushwaha et al. [20]. The purple membrane lipids were yellow due to retinal. Extracted lipids were dissolved in a small amount of chloroform and the solvent was evaporated under a gentle stream of nitrogen and then under vacuum. Lipid membranes were prepared by adding distilled water to the dried lipid and incubated for 2 h at room temperature. They were sealed in a thin-wall glass capillary as described above for X-ray studies.

2. X-ray diffraction studies

X-rays were generated by Rigaku Denki rotating-anode RU3HM or RU 100 microfocus generator with a copper target. RU3HM was operated at 55 kV and 5.8 mA and RU 100 at 40 kV and 25 mA. The focal size, viewed at 6° to the target surface, was about 100 μm × 100 μm. Ni-filtered CuKα radiation (wavelength 0.1542 nm (1.542 Å)) was used. The thickness of the Ni filter was 10 μm. Elliott toroidal focusing optics [21] was used with a set of double sector apertures.

Temperature of the specimen was adjusted by the gas flow around the capillary containing the specimen. Heated air was used for high temperatures and nitrogen gas belched out from liquid nitrogen was used for low temperatures. Temperature of the specimen was monitored by a copper-constantan thermocouple pasted on the capillary, which regulated a heater in the gas flow. The specimen temperature was controlled within ±0.5°C during X-ray exposure.

Diffraction patterns were recorded on Sakura cosmic ray film. The photographic density was measured with a Narumi (type C) microdensitometer. The absorbance was converted to the scattered X-ray intensity with the help of a standard scale. In lipid membranes, diffraction peak around 1/4.7 $Å^{-1}$ due to the packing of lipid hydrocarbon chains was measured with a position sensitive detector. The counter chamber was inclined by about 70° referring to the incident beam so as to make it perpendicular to the diffracted beam. Diffraction spacings were calibrated with sodium myristate powder. Most of X-ray path between the specimen and the film or the detector was evacuated to eliminate air scattering.

3. Absorption and CD spectra

The absorption and CD spectra were measured with Union SM401 spectrophotometer and Union Dichrograph Mark III J spectropolarimeter, respectively. In these measurements, the purple membrane was dispersed in distilled water and the brown holo-membrane in 1 mM Tris-HCl buffer (pH 6.4). Absorption and CD spectra were measured with a cell of 1 cm light path. Temperature of the cell holder was controlled within ±0.2°C by circulating water through a thermoregulator, Neslab RTE-8. The purple membrane was gently sonicated to reduce the light scattering in measuring CD spectrum. CD spectrum of distilled water was used as a reference. In the case of the brown holo-membrane, the spectrum of the brown apo-membrane was used as a reference to minimize the distortion due to light scattering artifact.

Results

1. X-ray diffraction patterns

(a) purple membrane. The partially hydrated specimens gave better oriented diffraction patterns but had higher transition temperatures than the fully hydrated specimens, which had the same transition temperature as the membranes dispersed in water. The X-ray data presented below were those obtained with the fully hydrated specimens.

Fig. 2A gives X-ray photographs of the purple membrane at 28, 74, 78 and 60°C. Temperature of the specimen was changed in the sequence of 28, 74, 78 and 60°C. The direction parallel to the plane of membranes is called equator and the perpendicular direction meridian. Fig. 2B shows the intensity distributions along the equator which were obtained by microdensitometer tracing of the photographs in Fig. 2A with corrections by the intensity scale. The abscissa is $1/d$, where d is the spacing given by $\lambda/2\sin\theta$), λ being the wavelength and 2θ being the scattering angle. Intensity curves are shifted from each other to avoid overlapping.

Fig. 2A shows that the Bragg reflection lines are still present at 74°C although the background becomes relatively high (b). The Bragg lines disappear at 78°C but there are diffuse peaks indicated by arrows (c), suggesting that some local order exists in arrangement of bacteriorhodopsin. It should be no-

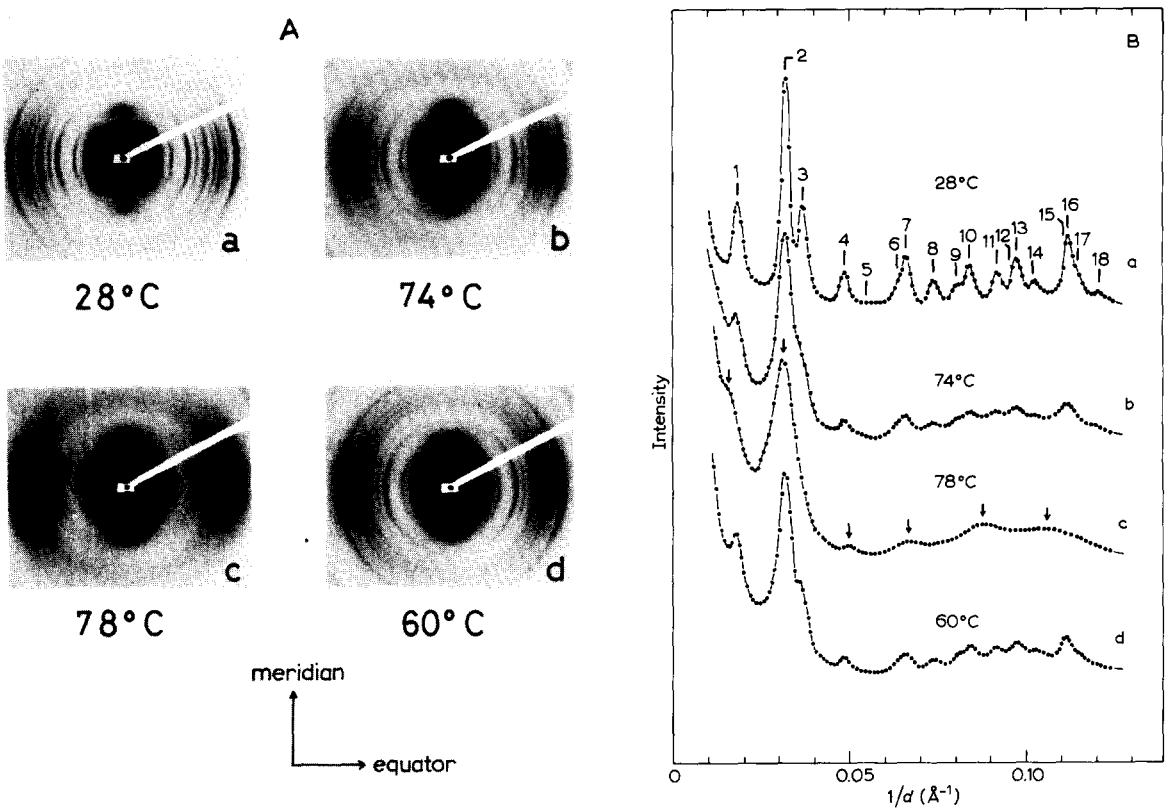

Fig. 2. A. X-ray diffraction photographs of oriented purple membrane at 28°C (a), 74°C (b), 78°C (c) and 60°C (d). Temperature was changed in the sequence of 28, 74, 78 and 60°C. Incident X-ray beam was parallel to the plane of membranes. Specimen-to-film distance was 9.0 cm. Exposure time: 1.5 h (a), 2 h (b), 9 h (c) and 3 h (d). B. Equatorial intensities obtained by microdensitometer tracings of the photographs in Fig. 2A with corrections by the intensity scale. The number on the curve a indicates the order of the diffraction peaks including non-observed ones.

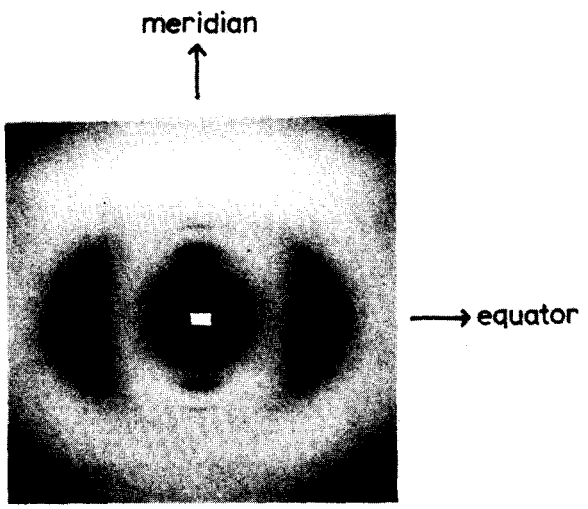

Fig. 3. X-ray diffraction photograph of the thermally denatured purple membrane. Incident X-ray beam was parallel to the plane of membranes. Specimen-to-film distance, 7.7 cm. Exposure time, 38 h.

ticed here that exposure times were different in taking the photographs as mentioned in the caption of Fig. 2A, and thus the peaks on the curve c in Fig. 2B will be much flatter than the Bragg peaks on the curves a, b and d if they are plotted in the absolute scale. Upon cooling back to 60°C, the Bragg lines reappeared. The recrystallization proceeded very slowly when the specimen was cooled from 78°C to 28°C, but it was nearly completed with 15 min at 60°C. Table I gives $1/d$ of the Bragg reflections on the curves a, b, d and the broad peaks on the curve c. The

lattice edge length a was determined as 62.7 Å at 28°C, 63.1 Å at 74°C and 63.1 Å at 60°C by using the d values in Table I. In the calculation d values of the first peak were not used at 74°C and 60°C since experimental errors seemed large for them.

Fig. 3 shows a diffraction photograph of the purple membrane after the heat treatment in boiling water. Only a broad peak appears around 1/10 $Å^{-1}$ along the equator, indicating that thermally denatured bacteriorhodopsin does not crystallize.

(b) Brown holo-membrane. Fig. 4A gives X-ray diffraction photographs of the brown holo-membrane at 28, 60 and 28°C after heating to 60°C. The Bragg reflections of the same type as the purple membrane appeared at 28°C (a), as reported previously [9]. They were absent at 60°C (b). Other photographs proved that the Bragg lines were still present at 50°C. Therefore, the transition temperature lies between 50°C and 60°C. The transition is reversible: the Bragg lines reappeared when the specimen was cooled from 60°C to 28°C (c). Fig. 4B shows intensity distributions along the equator obtained from the photographs. As seen in Fig. 4A, strong lamellar reflections appeared along the meridian at low angles. A tail of the lamellar reflection extended to the equator and seems to have caused some distortion to the intensity curves around the lowest-angle Bragg reflection at about 0.018 $Å^{-1}$ in Fig. 4B. Table II gives observed values of $1/d$ of the Bragg reflections at 28°C and the broad peaks at 60°C. The d values at 28°C could be well reproduced with a of 62.8 Å, except for the first peak on which the lamellar reflection was overlapped.

TABLE I

OBSERVED $1/d$ OF EQUATORIAL REFLECTIONS BY THE PURPLE MEMBRANE

$1/d$ ($Å^{-1}$)				
Bragg reflection				Non-Bragg reflection
Order [a]	28°C	74°C	60°C (after heating to 78°C)	78°C
				0.016
1	0.0184	0.0174	0.0176	
				0.0314
2	0.0319	0.0319	0.0316	
3	0.0370			
4	0.0487	0.0483	0.0482	
				0.0497
7	0.0661	0.0658	0.0655	
				0.0668
8	0.0739	0.0732	0.0738	
9	0.0805			
10	0.0841	0.0841	0.0841	
				0.0877
11	0.0920	0.0913	0.0913	
13	0.0972	0.0971	0.0971	
14	0.1022		0.1026	
				0.106
16	0.1119	0.1113	0.1110	

[a] Theoretically expected order of the Bragg reflection.

TABLE II

OBSERVED $1/d$ OF EQUATORIAL REFLECTIONS BY THE BROWN HOLO-MEMBRANE

$1/d$ ($Å^{-1}$)			
Bragg reflection			Non-Bragg reflection
Order [a]	28°C	28°C (after heating to 60°C)	60°C
1	0.0182 [b]	0.0182 [b]	
			0.026
2	0.0320	0.0319	
3	0.0367	0.0366	
4	0.0485	0.0486	0.0485
7	0.0662	0.0662	
			0.0671
8	0.0737	0.0740	
9	0.0803	0.0802	
10	0.0842	0.0841	
			0.0873
11	0.0921	0.0921	
13	0.0976	0.0973	
			0.106
16	0.1119	0.1120	

[a] Theoretically expected order of the Bragg reflection.
[b] Overlapped by a lamellar reflection.

2. Absorption spectrum

Visible absorption spectra of the purple membrane and the brown holo-membrane were measured between 19 and 88°C. Fig. 5A shows λ_{max}, the wave-

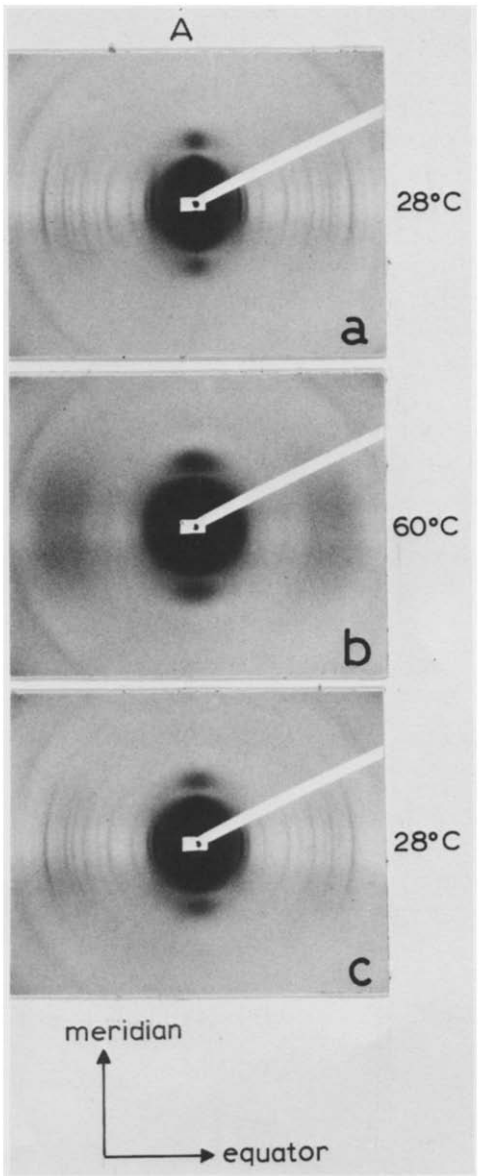

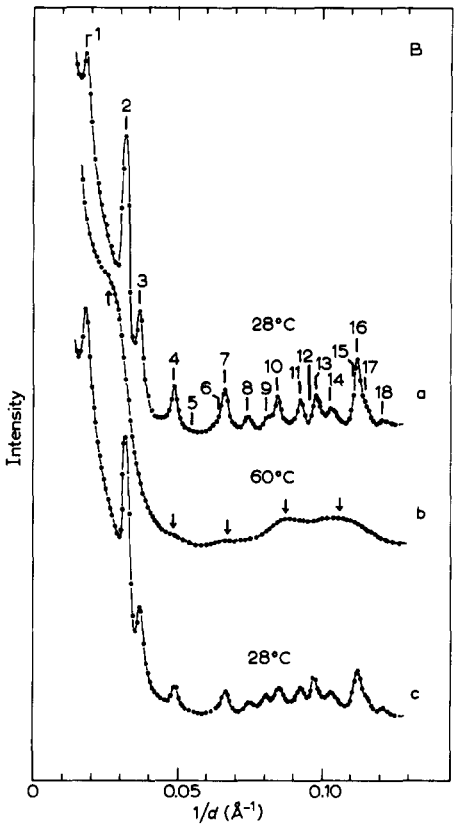

Fig. 4. A. X-ray diffraction photographs of the brown holo-membrane at 28°C (a), 60°C (b) and 28°C after heating to 60°C (c). Temperature of the specimen was changed in the sequence of 28, 60 and 28°C. Incident X-ray beam was parallel to the plane of membranes. Specimen-to-film distance, 8.7 cm. Exposure time: 6 h (a), 6 h (b) and 10 h (c). The white band along the equator is a shadow of the capillary in the air background scattering. B. Equatorial intensities obtained by microdensitometer tracing of the photographs in A with corrections by the intensity scale. The number on the curve a indicates the order of the diffraction peaks including non-observed ones.

length where the absorbance becomes maximal, as a function of temperature. Fig. 5B shows A_{max}, the absorbance at λ_{max}. Both λ_{max} and A_{max} decrease with increasing temperature and sharply drop around 80°C, as reported by Jackson and Sturtevant for the purple membrane [14]. Upon cooling back to room temperature from 80°C, λ_{max} returned to the original value of 560 nm, but A_{max} was a little smaller than the original value as reported by Jackson and Sturtevant [14]. The difference was about 0.5% in both the purple membrane and the brown holo-membrane. The curve a in Fig. 5B shows that the drop of A_{max} is sharper just below 78°C than just above 78°C. This feature was observed to be reproducible in repeated measurements.

3. CD spectra

Fig. 6A demonstrates visible CD spectra of the purple membrane dispersed in water at 26, 78 and

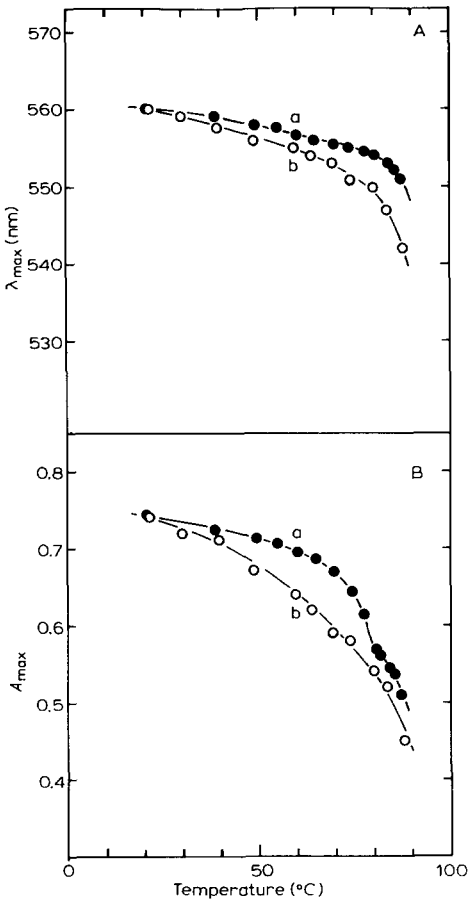

Fig. 5. Temperature dependence of the absorption spectra of the purple membrane (a) and the brown holo-membrane (b). A. Wavelength of absorption maximum, λ_{max}. B. Absorbance at λ_{max}, A_{max}.

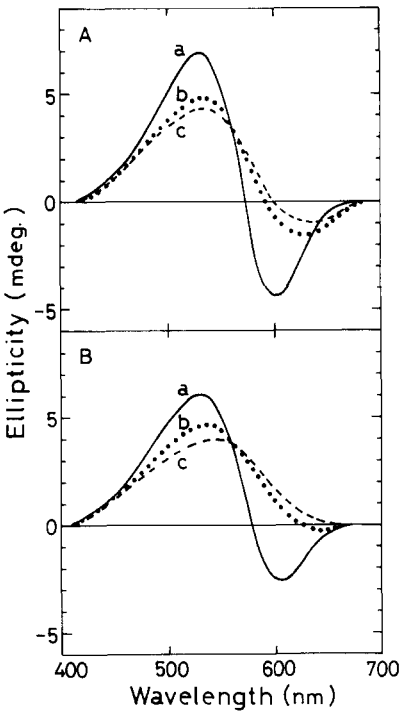

Fig. 6. Visible CD spectra. Ellipticity per 15.9 μM of bacteriorhodopsin is given. A. Purple membrane at 26°C (a), 78°C (b) and 80°C (c). B. Brown holo-membrane at 26°C (a), 60°C (b) and 70°C (c).

80°C. The spectrum at 26°C is bilobed though asymmetric, consisting of a positive band around 530 nm and a negative band around 605 nm (a), as reported by others [22–25]. With increasing temperature, the negative band diminishes more drastically than the positive band (b, c), but is still observed at 80°C (c), i.e., above the transition temperature. The spectrum returned to the original shape when the specimen was cooled back to 26°C.

Fig. 6B shows visible CD spectra of the brown holo-membrane at 26, 60 and 70°C. The asymmetry is larger than for the purple membrane at 26°C (a). The negative band becomes very small at 60°C (b)

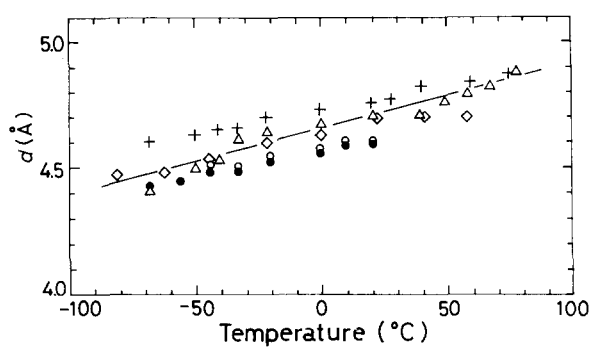

Fig. 7. The spacing d of the diffraction peak around 0.213 $Å^{-1}$ by membranes of lipids extracted from the purple membrane as a function of temperature. The peak is related with the side-by-side packing of the hydrocarbon chains of lipids. The different symbols correspond to different runs of experiments.

and disappears at 70°C. The spectrum returned to the original shape upon cooling back to 26°C.

4. X-ray studies of lipid membranes

X-ray diffraction studies were made on membranes of the total lipids extracted from the purple membrane. Our main concern was whether there were any phase transitions concerning the arrangement of the hydrocarbon chains, and diffraction pattern around 1/4.7 $Å^{-1}$ was investigated as a function of temperature between –81°C and 77°C. Only a broad peak was observed in the whole temperature range. Fig. 7 shows the spacing d of the broad peak as a function of temperature. Five series of experiments were carried out, and the results are shown by different marks in Fig. 7. The spacing d depends upon temperature linearly within the experimental error.

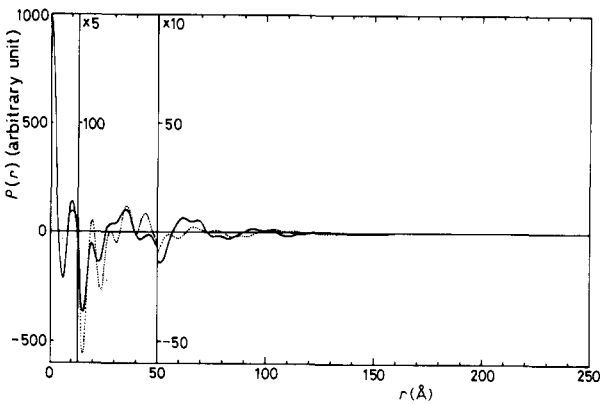

Fig. 8. Radial autocorrelation functions $P(r)$ for the purple membrane at 78°C (solid line) and for the brown holo-membrane at 60°C (dotted line). Equatorial intensities from 0.0218 to 0.141 $Å^{-1}$ in $1/d$ were used to calculate $P(r)$ for both membranes.

Discussion

1. Phase transitions and local orders above the transition temperature

In the present study we have confirmed the idea of Jackson and Sturtevant [14] that the '80°C' transition of the purple membrane involves a reversible and cooperative change of the crystalline structure of bacteriorhodopsin. In our specimens, the crystal to liquid transition occurred around 74–78°C in the purple membrane and around 50–60°C in the brown holo-membrane.

A weak phase transition was observed at about 30°C in the purple membrane through DSC measurements [26], with spin-labeled probes [27] and fluorescent probes [28]. Now it is certain that the weak transition is not related with disappearance of the hexagonal lattice.

As noticed in Results, the peak indicated by the arrows in Fig. 2B(c) (78°C) and 4B(b) (60°C) should be much flatter than the Bragg peaks of the other curves if all the curves are plotted in a common scale. These broad peaks suggest that some local order is present in molecular arrangement above the transition point although the crystalline long range order disappeared. The radial autocorrelation function $P(r)$, the Fourier transform of the observed equatorial intensity, was calculated to estimate extension of the local order, as was done in the reference [29]. Fig. 8 shows the results for the purple membrane (solid line) and for the brown holo-membrane (dotted line), as functions of the radial coordinate r in the cylindrical coordinate system. In both membranes $P(r)$ has a large amplitude for $r < 60$ Å and tends to zero at about 120 Å. The structure of the purple membrane determined by Unwin and Henderson [5], of which a rough sketch is shown in the inset of Fig. 9, seems to give the impression that trimers of bacteriorhodopsin are constitutional unit of the hexagonal lattice. Therefore, we speculated that such a trimer structure persists above the transition temperature, so that $P(r)$ has the large amplitude for $r < 60$ Å. $P(r)$ may have non-zero values up to 120 Å if there is a correlation in arrangement of neighbouring trimers. Then the diffraction pattern may have features similar to those by polystyrene latex spheres observed with soft X-rays [30]. That is, the pattern in the very small angle region will be governed by inter-trimer interference and that in the small to medium angle region will reflect intra-trimer interference. Thus we have examined whether the main feature of the curve c in Fig. 2B can be approximately reproduced by diffraction pattern by a single trimer in the small to medium angle region. We have approximated the contour map given by Unwin and Henderson [5] by sum of eight Gaussian functions, of which positions are shown by black circles in the 'monomer' in the top of Fig. 9. Diffraction intensities were calculated by the equations derived by Oster and Riley [31], for the mono-

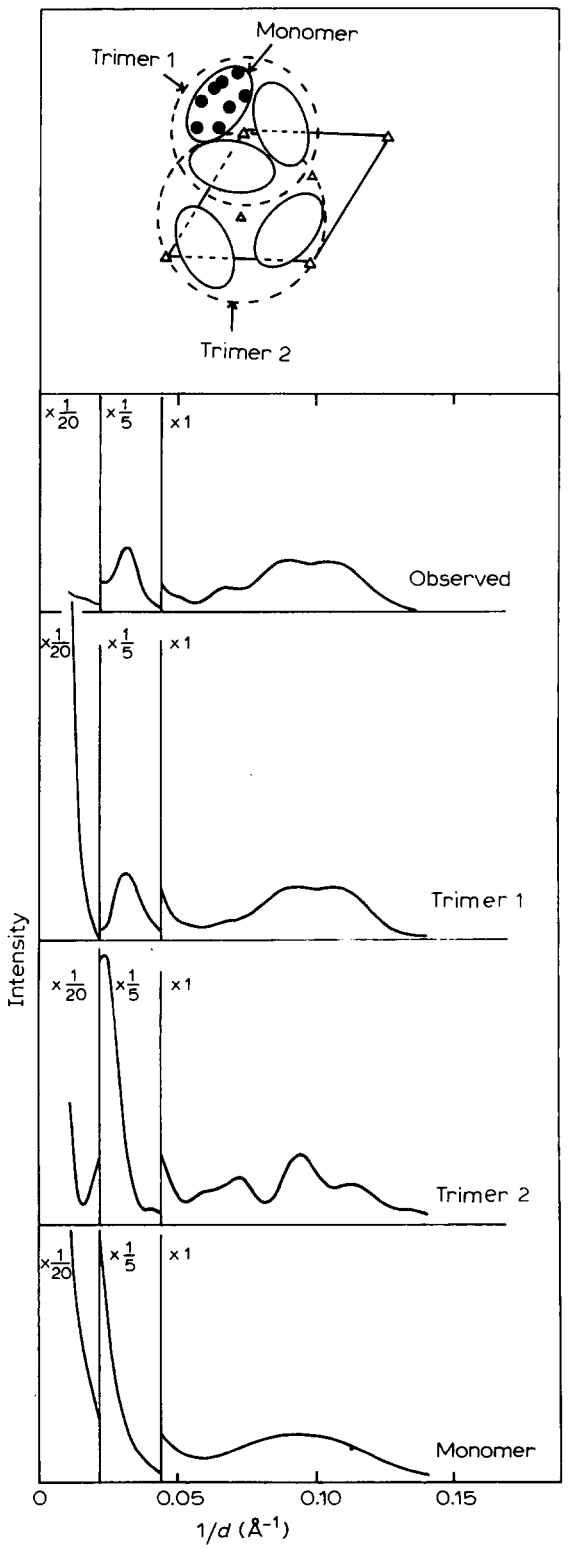

mer, the trimer 1 and the trimer 2 indicated in the inset. Results are given in Fig. 9, in comparison with the observed values, which were derived from the curve c in Fig. 2B, with background subtraction on the assumption that it was flat and equal to the intensity at $1/d$ of 0.14 $Å^{-1}$ and with the Lorentz correction by the factor $\lambda/(2\sin\theta)$. Calculated curves in Fig. 9 were normalized so that the trimer 1 gives the same value at $1/d = 0.09$ $Å^{-1}$ as observed. One can see in Fig. 9 that the trimer 1 gives a diffraction pattern quite similar to the observed one, whereas the trimer 2 and the monomer do not. Especially the trimer 1 gives the first peak at 0.031 $Å^{-1}$ close to the observed peak position (0.0314 $Å^{-1}$) but the trimer 2 gives the first peak at 0.024 $Å^{-1}$. The monomer gives only smooth intensity distribution. Therefore, bacteriorhodopsin molecules seem to be in the mode of the trimer 1 just above the transition temperature. This single trimer model, however, does not explain the features of the observed curve in the very small angle as expected. It gives a wider peak at the origin and does not give the small bump observed around 0.016 $Å^{-1}$ (cf. Fig. 2B(c)). The observed features should be attributed to the inter-trimer interference. These results are quite similar to the case of latex spheres, as seen in Fig. 6 of the reference [30].

The negative band in the CD spectrum is regarded as a measure of exciton coupling in molecular assembly of bacteriorhodopsin [32]. Thus such local order as the trimer will cause the exciton coupling and thus the negative CD band. Fig. 6 demonstrates that the negative band of the CD spectrum persist just above the transition temperature, as seen in the dotted curves b at 78°C in Fig. 6A and at 60°C in Fig. 6B. The dashed curves c at 80°C in Fig. 6A and at 70°C in Fig. 6B suggest that the local order diminishes at high temperatures.

Fig. 9. X-ray intensity distributions along the equator. Observed: the intensity distribution by the purple membrane at 78°C. Other curves: calculated for the models of the trimer 1, the trimer 2 and the monomer shown. Top: Projection of the purple membrane structure. 'Monomer' corresponds to an assumed bacteriorhodopsin molecule. Black circles stand for the Gaussian functions which were used for approximate expression of the structure. Triangle represents the axis of 3-fold rotational symmetry.

2. Temperature dependence of absorption spectrum

Jackson and Surtevant observed that both λ_{max} and A_{max} dropped sharply around 80°C in the purple membrane [14], as reconfirmed by the curves a in Fig. 5. The curves b in Fig. 5 show similar changes around 80°C in the brown holo-membrane of which the transition point lies between 50°C and 60°C. Therefore, it may be concluded that substantially the spectrum changes are not caused by the phase transition. Fischer and Oesterhelt [33] discussed on a conformational change of the protein moiety around the retinal at high temperature and proposed formation of '500 nm chromophore'. The differences between the curves a and b in Fig. 5, however, are appreciable. They seem to be caused at least partly by the difference between the phase transition temperatures. The curve a in Fig. 5B shows that the drop of A_{max} is sharper just below 78°C than just above it, indicating an effect of the phase transition.

3. Difference between properties of the purple membrane and the brown holo-membrane

As cited in Introduction several authors noticed the differences between the behaviours of bacteriorhodopsin molecules in the purple membrane and the brown holo-membrane; on the rotational motion [11, 12] and light-dark adaptation [7,13]. In the present study we have observed that the phase transition takes place about 20°C lower in the brown holo-membrane than in the purple membrane. Fig. 5 shows that the spectral change occurs at lower temperatures in the brown holo-membrane than in the purple membrane. Fig. 6 indicates that the exciton coupling decreases at lower temperatures in the brown holo-membrane than in the purple membrane. The dashed curve (c) in Fig. 6B suggests that bacteriorhodopsin becomes almost monomeric at 70°C in the brown holo-membrane.

The density of the brown holo-membrane is 1.14 g/cm^3 [6] compared to 1.18 g/cm^3 of the purple membrane [1], suggesting the molar ratio of lipids are larger in the brown holo-membrane than in the purple membrane. Also the brown holo-membrane contains cytochrome *b*-type proteins as well as other minor proteins. Therefore, one may speculate that molecules other than bacteriorhodopsin get into the hexagonal lattice as impurities in the brown holo-membrane. The lattice constants a at 28°C determined from the d values in Table I and II are, however, the same, 62.7 Å for the purple membrane and 62.8 Å for the brown holo-membrane in agreement with our previous result [9]. The integral width w of the Bragg peak depended upon $1/d$ approximately by $w = \alpha + \beta(1/d)$, where α and β are constants. β was common for the two membranes but α was 27% larger for the brown holo-membrane than the purple membrane. This fact suggests that size of the single crystal region is smaller in the brown holo-membrane than in the purple membrane. Rough estimation of the diameter of the region was made by using values of α and the Scherrer formula (cf. §5.1 of Ref. 34), with the result of $16a$ for the brown holo-membrane, where a is the cell edge length.

Jackson and Sturtevant observed that the transition temperature was lowered when the purple membrane were contaminated by the red membranes [14]. The low transition temperature (50–60°C) of the brown holo-membrane seems to be an analogous phenomenon since the membrane contains the cytochrome *b*-type protein and the minor proteins. It might be a possibility that the phase transition corresponds to dissolution of the hexagonal lattice associated with mixing of bacteriorhodopsin with other proteins in the brown holo-membrane whereas it is simple melting of the hexagonal lattice in the purple membrane.

4. Membranes of extracted lipids

Jackson and Sturtevant [35] did DSC measurements on membranes of the extracted lipids from the purple membrane above 0°C but found no anomaly. Purple membrane lipids are thought to contain exclusively dihydrophytol chains ether linked to glycerol [36]. Lindsey et al. [37] did DSC studies on the synthetic lipid, diphytanoylphosphatidylcholine which has dihydrophytol chains, but did not find any phase transition between −120°C and 120°C. Our X-ray studies have proved that the membrane of the extracted lipid remains in a disordered phase between −81°C and 77°C, supporting the results by Jackson and Sturtevant [35] and by Lindsey et al. [37].

The lipids have hydrocarbon chains, each having four methyl side chains. Fig. 7 shows that d at 40°C is about 4.76 Å, compared to 4.5 Å of the extracted lipids from *Escherichia coli* [38], and indicates that the average thickness of the branched chain is larger

than the non-branched ones. Also the half width of the 4.7 Å peak was about 40% larger than the 4.5 Å peak of *E. coli,* suggesting more disordered arrangement of the branched chains. The linear thermal expansion coefficient $((\Delta d/d)/\Delta T)$ estimated from Fig. 7 is $0.56 \cdot 10^{-3}$ K^{-1} which may be compared with that of paraffin, $0.48 \cdot 10^{-3}$ K^{-1} between 38°C and 49°C [39].

References

1 Stoeckenius, W. and Kunau, W.H. (1968) J. Cell Biol. 38, 337–357
2 Oesterhelt, D. and Stoeckenius, W. (1971) Nature New Biol. 233, 149–152
3 Oesterhelt, D. and Stoeckenius, W. (1973) Proc. Natl. Acad. Sci. USA 70, 2853–2857
4 Blaurock, A.E. and Stoeckenius, W. (1971) Nature New Biol. 233, 152–155
5 Unwin, P.N.T. and Henderson, R. (1975) J. Mol. Biol. 94, 425–440
6 Sumper, M., Reitmeier, H. and Oesterhelt, D. (1976) Angew. Chem. Int. Ed. Engl. 15, 187–194
7 Papadopoulos, G.K. and Cassim, J.Y. (1979) Biophys. J. 25, 311a
8 Sumper, M. and Herrmann, G. (1976) FEBS Lett. 69, 149–152
9 Hiraki, K., Hamanaka, T., Mitsui, T. and Kito, Y. (1978) Biochim. Biophys. Acta 536, 318–322
10 Neugebauer, D.-C., Zingsheim, H.P. and Oesterhelt, D. (1978) J. Mol. Biol. 123, 247–257
11 Razi Naqvi, K., Gonzalez-Rodriguez, J., Cherry, R.J. and Chapman, D. (1973) Nature New Biol. 245, 249–251
12 Cherry, R.J., Heyn, M.P. and Oesterhelt, D. (1977) FEBS Lett. 78, 25–30
13 Peters, R. and Peters, J. (1978) in Energetics and Structure of Halophilic Microorganisms (Caplan, S.R. and Ginzburg, M., eds.), pp. 315–321, Elsevier/North-Holland Biomedical Press, Amsterdam
14 Jackson, M.B. and Sturtevant, J.M. (1978) Biochemistry 17, 911–915
15 Oesterhelt, D. and Stoeckenius, W. (1974) Methods Enzymol. 31, 667–678
16 Hiraki, K., Hamanaka, T., Mitsui, T. and Kito, Y. (1981) Photochem. Photobiol. 33, 429–433
17 Lowry, O.H., Rosebrough, N.J., Farr, A.L. and Randall, R.J. (1951) J. Biol. Chem. 193, 265–275
18 Rehorek, M. and Heyn, M.P. (1979) Biochemistry 18, 4977–4983
19 (1976–1977) in Handbook of Chemistry and Physics (Weast, R.C., ed.), 57th edn., p. E-46, Chemical Rubber Co., Cleveland, OH
20 Kushwaha, S.C., Kates, M. and Martin, W.G. (1975) Can. J. Biochem. 53, 284–292
21 Elliott, A. (1965) J. Sci. Instrum. 42, 312–316
22 Heyn, M.P., Bauer, P.-J. and Dencher, N.A. (1975) Biochem. Biophys. Res. Commun. 67, 897–903
23 Becher, B. and Cassim, J.Y. (1976) Biophys. J. 16, 1183–1200
24 Kriebel, A.N. and Albrecht, A.C. (1976) J. Chem. Phys. 65, 4575–4583
25 Ebrey, T.G., Becher, B., Mao, B., Kilbride, P. and Honig, B. (1977) J. Mol. Biol. 112, 377–397
26 Degani, H., Bach, D., Danon, A., Garty, H., Eisenbach, M. and Caplan, S.R. (1978) in Energetics and Structure of Halophilic Microorganisms (Caplan, S.R. and Ginzburg, M., eds.), pp. 225–232, Elsevier/North-Holland Biomedical Press, Amsterdam
27 Chignell, C.F. and Chignell, D.A. (1975) Biochem. Biophys. Res. Commun. 62, 136–143
28 Korenstein, R., Sherman, W.V. and Caplan, S.R. (1976) Biophys. Struct. Mech. 2, 267–276
29 Kataoka, M. and Ueki, T. (1980) Acta Cryst. A36, 282–287
30 Wakabayashi, K., Kakizaki, A., Siota, Y., Namba, K., Kurita, K., Yokata, M., Tagawa, H., Inoko, Y., Mitsui, T., Wada, E., Ueki, T., Nagakura, I. and Matsukawa, T. (1978) J. Phys. Soc. Japan 44, 1314–1322
31 Oster, G. and Riley, D.P. (1952) Acta Cryst. 5, 272–276
32 Cherry, R.J., Müller, U., Henderson, R. and Heyn, M.P. (1978) J. Mol. Biol. 121, 283–298
33 Fischer, U. and Oesterhelt, D. (1979) Biophys. J. 28, 211–230
34 Guinier, A. (1963) in X-ray Diffraction in Crystals, Imperfect Crystals and Amorphous Bodies (translated in English by Lorrain, P. and Lorrain, D.S.-M.), Freeman, W.H.
35 Jackson, M.B. and Sturtevant, J.M. (1978) Biochemistry 17, 4470–4474
36 Kates, M., Yengoyan, L.S. and Sastry, P.S. (1965) Biochim. Biophys. Acta 98, 252–268
37 Lindsey, H., Petersen, N.O. and Chan, S.I. (1979) Biochim. Biophys. Acta 555, 147–167
38 Nakayama, H., Mitsui, T., Nishihara, M. and Kito, M. (1980) Biochim. Biophys. Acta 601, 1–10
39 (1962–1963) in Handbook of Chemistry and Physics (Hodgman, C.D., ed.), 44th edn., p. 2328, Chemical Rubber Co., Cleveland, OH